Proceeding Series of the Brazilian Society of Applied and Computational Mathematics, Vol. 5, N. 1, 2017.

Trabalho apresentado no CNMAC, Gramado - RS, 2016.

**Proceeding Series of the Brazilian Society of Computational and Applied Mathematics**

# Solving hyperbolic conservation laws by using Lagrangian-Eulerian approach

Eduardo Abreu[1]
Institute of Mathematics, Statistics and Scientific Computing IMECC - UNICAMP, Campinas, SP
John A. Perez S.[2]
Facultad de Ciencias ITM Institución Universitaria, Medellín, Colombia.
Institute of Mathematics, Statistics and Scientific Computing IMECC - UNICAMP, Campinas, SP
Arthur M. E. Santo[3]
Institute of Mathematics, Statistics and Scientific Computing IMECC - UNICAMP, Campinas, SP

**Abstract**. We discuss a procedure for numerically solving nonlinear hyperbolic conservation law problems by means of a Lagrangian-Eulerian framework. The underlying hyperbolic conservation law is written in a space-time divergence form, so that inherent conservation properties of the problem are reflected in the numerical scheme. In order to enhance resolution and accuracy of the approximations, we make use of polynomial reconstruction ideas into the Lagrangian-Eulerian novel approach. Finally, numerical results are given to verify the formal construction as well as to demonstrate its accuracy, efficiency, and versatility. These results for the considered sample problems compare very well to analytical results.

**Keywords**. Conservation laws, Lagrangian-Eulerian, Finite Volume Methods

## 1 Introduction

In this work we present a numerical scheme for solving hyperbolic conservation laws by means of a Lagrangian-Eulerian approach. This framework has been used for numerically solving partial differential equations of several types, such as hyperbolic conservation laws [8,11], balance laws problems [3,6] and parabolic equations [4]. In the work [4], it was identified the region in the space-time domain where the mass conservation takes place, but linked to a scalar convection-dominated nonlinear parabolic problem, which models the immiscible incompressible two-phase flow in a porous medium [1]. Some similar developments based on Lagrangian-Eulerian framework, with focus on increasing order and accuracy of such schemes can be found in [6]. More recently in [2, 11], such ideas were extended to a wide range of nonlinear purely hyperbolic conservation laws and balance laws – scalar and systems. Our goal on the current work is to present the formal construction of an accurate Lagrangian-Eulerian scheme for hyperbolic conservation laws. Preliminary results showed qualitatively correct solutions with accurate resolution.

[1]eabreu@ime.unicamp.br
[2]jhonperez@itm.edu.co
[3]arthurm@ime.unicamp.br

 

## 2 Numerical Method

Consider the following hyperbolic conservation law for $u = u(x,t)$

$$\frac{\partial u}{\partial t} + \frac{\partial H(u)}{\partial x} = 0, \quad x \in \mathbb{R},\, t > 0 \qquad u(x,0) = \eta(x), \quad x \in \mathbb{R}. \tag{1}$$

We provide a formal development of the analogue Lagrangian-Eulerian scheme [2–4, 11] for numerically solving the initial value problem with $x \in \mathbb{R}$, $t > 0$. As in the Lagrangian-Eulerian schemes [3, 4], local conservation is obtained by integrating the conservation law over the region in the space-time domain where the conservation of the mass flux takes place. Consider the Lagrangian-Eulerian finite-volume cell centers

$$D_j^n = \{(t,x) \;/\; t^n \le t \le t^{n+1},\; \sigma_{j-\frac{1}{2}}(t) \le x \le \sigma_{j+\frac{1}{2}}(t)\}, \tag{2}$$

where $\sigma^n_{j-\frac{1}{2}}(t)$ is the parameterized integral curve such that $\sigma^n_{j-\frac{1}{2}}(t^n) = x^n_{j-\frac{1}{2}}$. These curves are the lateral boundaries of the domain $D_j^n$ in (2) and we define $\bar{x}^{n+1}_{j-\frac{1}{2}} := \sigma^n_{j-\frac{1}{2}}(t^{n+1})$ and $\bar{x}^{n+1}_{j+\frac{1}{2}} := \sigma^n_{j+\frac{1}{2}}(t^{n+1})$ as their endpoints in time $t^{n+1}$. The numerical scheme is expected to satisfy some type of mass conservation (due to the inherent nature of the conservation law) from time $t^n$ in the space domain $\left[x^n_{j-\frac{1}{2}}, x^n_{j+\frac{1}{2}}\right]$ to time $t^{n+1}$ in the space domain $\left[\bar{x}^{n+1}_{j-\frac{1}{2}}, \bar{x}^{n+1}_{j+\frac{1}{2}}\right]$. With this, we must have the flux through curves $\sigma^n_{j-\frac{1}{2}}(t)$ to be zero. From the integration of (1) and the divergence theorem, using the fact that the line integrals over curves $\sigma^n_j(t)$ vanish, we get

$$\int_{\bar{x}^{n+1}_{j-\frac{1}{2}}}^{\bar{x}^{n+1}_{j+\frac{1}{2}}} u(x,t^{n+1})dx = \int_{x^n_{j-\frac{1}{2}}}^{x^n_{j+\frac{1}{2}}} u(x,t^n)dx. \tag{3}$$

The linear case from [3] is essentially imitated, but here the curves $\sigma^n_{j-1/2}(t)$ are not straight lines in general, but rather solutions of the set of local nonlinear differential equations [3, 11]: $\frac{d\sigma^n_{j-1/2}(t)}{dt} = \frac{H(u)}{u}$, for $t^n < t \le t^{n+1}$, with the initial condition $\sigma^n_{j-1/2}(t^n) = x^n_{j-1/2}$, assuming $u \neq 0$ (for the sake of presentation).

The extension of this construction follows naturally from the finite volume formulation of the linear Lagrangian-Eulerian scheme as building block to construct *local* approximations such as $f^n_{j-1/2} = \frac{H(U^n_{j-1/2})}{U^n_{j-1/2}} \approx \frac{H(u)}{u}$ with the initial condition $\sigma^n_{j-1/2}(t^n) = x^n_{j-1/2}$. Indeed, distinct and high-order approximations are also acceptable for $\frac{d\sigma^n_{j-1/2}(t)}{dt}$ and can be viewed as ingredients to improve accuracy of the new family of Lagrangian-Eulerian methods; this will be addressed later. Equation 3 defines conservation of mass but in a different mesh cell-centered in points $\bar{x}^n_{j+\frac{1}{2}}$. We will later address how to project these volumes back to the original mesh. The piecewise constant numerical data is reconstructed into a piecewise linear approximation (but high-order reconstructions are acceptable), through the use of MUSCL-type interpolants:

$$L_j(x,t) = u_j(t) + (x - x_j)\frac{1}{\Delta x}u'_j. \tag{4}$$

DOI: 10.5540/03.2017.005.01.0329  

For the numerical derivative $\frac{1}{\Delta x}u'_j$ , there are several choices of slope limiters; in book [8] there is a good compilation of many options; a priori choice of such slope limiters is quite hard, but they are chosen upon the underlying model problem under investigation. One possible for the slope limiter is

$$U'_j = MM\left\{\alpha\Delta u_{j+\frac{1}{2}}, \frac{1}{2}(u_{j+1}-u_{j-1}), \alpha\Delta u_{j-\frac{1}{2}}\right\}, \tag{5}$$

and this choice for slope limiter allows steeper slopes near discontinuities and retain accuracy in smooth regions. The range of the parameter $\alpha$ is typically guided by the CFL condition [9]. Here, $MM$ stands for the usual MinMod limiter [8,9], with $\Delta u_{j+\frac{1}{2}} = u_{j+1} - u_j$,

$$MM\{\sigma,\tau\} = \frac{1}{2}\left[sgn(\sigma)+sgn(\tau)\right]\min\left\{|\sigma|,|\tau|\right\}. \tag{6}$$

The discrete version of equation (3), using the piecewise linear approximation above, is

$$\overline{U}_j^{n+1} = \frac{1}{h_j^{n+1}}\int_{\bar{x}_{j-\frac{1}{2}}^{n+1}}^{\bar{x}_{j+\frac{1}{2}}^{n+1}} u(x,t^{n+1})dx = \frac{1}{h_j^{n+1}}\int_{x_{j-\frac{1}{2}}^{n}}^{x_{j+\frac{1}{2}}^{n}} u(x,t^{n})dx = \frac{h}{h_j^{n+1}}U_j^n, \tag{7}$$

in which we use the approximations

$$\overline{U}_j^{n+1} := \frac{1}{h_j^{n+1}}\int_{\bar{x}_{j-\frac{1}{2}}^{n+1}}^{\bar{x}_{j+\frac{1}{2}}^{n+1}} u(x,t^{n+1})dx, \quad \text{and} \quad U_j^n := \frac{1}{h}\int_{x_{j-\frac{1}{2}}^{n}}^{x_{j+\frac{1}{2}}^{n}} u(x,t^{n})dx.$$

Solutions $\sigma_{j-1/2}^n(t)$ of the differential system are obtained using the approximations

$$\begin{aligned} U_{j-\frac{1}{2}} &= \frac{1}{h}\int_{x_{j-1}^n}^{x_j^n} L(x,t)dx = \frac{1}{h}\left(\int_{x_{j-1}^n}^{x_{j-\frac{1}{2}}^n} L_{j-1}(x,t)dx + \int_{x_{j-\frac{1}{2}}^n}^{x_j^n} L_j(x,t)dx\right) \\ &= \frac{1}{2}(U_{j-1}+U_j) + \frac{1}{8}(U'_j - U'_{j-1}). \end{aligned} \tag{8}$$

The above approximation is not necessary in the linear case where $H(u) = a(x,t)\,u$. We must notice that the approximation of $f_{j-1/2}^n$ may cause spurious oscillation in Riemann problems, specially in shocks and discontinuity regions (see Figure 2 in Section 3). For that, we use a polynomial reconstruction of second degree to smooth out the approximation. The numerical solutions have shown qualitatively correct behavior for nonlinear hyperbolic conservation laws. The convergence order remains unchanged even with the reconstruction, being a first-order approximation. In the reconstruction we use the nonlinear Lagrange polynomial in $U_{j-1}$, $U_j$ and $U_{j+1}$. So, equation (7) reads

$$\overline{U}_j^{n+1} = \frac{1}{h_j^{n+1}}\int_{x_{j-\frac{1}{2}}^{n}}^{x_{j+\frac{1}{2}}^{n}} P_2(x)dx, \tag{9}$$

DOI: 10.5540/03.2017.005.01.0329  

where $P_2(x) = U_{j-1}^n\, L_{-1}(x - x_j) + U_j^n\, L_0(x - x_j) + U_{j+1}^n\, L_1(x - x_j)$ and

$$L_{\pm 1}(x) = \frac{1}{2}\left[\left(\frac{x}{h} \pm \frac{1}{2}\right)^2 - \frac{1}{4}\right], \qquad L_0(x) = 1 - \left(\frac{x}{h}\right)^2. \tag{10}$$

Next, we obtain the resulting projection formula as follows

$$U_j^{n+1} = \frac{1}{h}\left(C_l \overline{U}_{j-1}^n + (h - C_l - C_r)\overline{U}_j^n + C_r \overline{U}_{j+1}^n\right), \tag{11}$$

where the projection coefficients are: $C_l = \frac{1}{2}\, f_{j-1/2}^n\, \Delta t^n (1 + sign(f_{j-1/2}^n))$ and $C_r = \frac{1}{2}\, |f_{j+1/2}^n|\, \Delta t^n (1 - sign(f_{j+1/2}^n))$. Here $\Delta t^n$ is obtained under CFL-condition

$$\max_j \left\{ |f_{j-\frac{1}{2}}\, \Delta t^n| \right\} \leq \frac{h}{2},$$

which is taken by construction of method. We note that in the linear case, when $a(x,t) = a > 0$ (or $a < 0$), the numerical scheme (7)-(11) is a generalization of the Upwind scheme, but our scheme can approximate solution in both cases $a > 0$ and $a < 0$, the CFL-condition in this case is $|a\, \Delta t| \leq h$ as in the Upwind scheme.

## 3 Numerical Experiments

We present and discuss computations for scalar linear and nonlinear conservation laws with convex and non-convex flux functions. In Figure 1, it is shown numerical solutions for $u_t + (a(x,t)\, u)_x = 0$ along with various $a(x,t)$ functions. For instance on the left picture we take a standard test case, called Shu's linear test [6, 7] with $a(x,t) = 0.5$ and 256 cells. On the center picture we show a test of our scheme on the case with $a(x,t) = \sin(x)$ over $[0, 2\pi]$, 128 cells and with the exact solution (see [6])

$$u(x,t) = \frac{\sin(2\, \arctan(e^{-t}\, \tan(x/2)))}{\sin(x)}.$$

And on the right picture of Figure 1 as in [6], we test a case with $a(x,t) = \sin(t)$ on $[0, 2]$ and 256 cells, for which the exact solution is $u(x,t) = u_0(x + 1 + cos(t))$ where $u_0(x) = 0.75 + 0.25 \sin(\pi\, x)$ over $[0, 2]$ simulated at time $t = 4$. Second and third cases present different velocity signals in space (center case) and over time (right case), and our method shows robustness by not needing any special treatment for that. In Figure 2, we present the solutions of the problem with Burgers' flux function $u_t + (u^2/2)_x = 0$ along with discontinuous initial data $u(x,0) = 1$, $x < 0$ and $u(x,0) = 0$, $x > 0$ (left picture), and $u(x,0) = -1$, $x < 0$ and $u(x,0) = 1$, $x > 0$ (right picture), without the reconstruction. The shock discontinuity on the left exhibits spurious oscillations. The right picture is a transonic rarefaction wave. In Figure 3, it is shown again the numerical solutions for $u_t + (u^2/2)_x = 0$ along with same discontinuous initial data $u(x,0) = 1$, $x < 0$ and $u(x,0) = 0$, $x > 0$ (left picture), and $u(x,0) = -1$, $x < 0$ and $u(x,0) = 1$,

DOI: 10.5540/03.2017.005.01.0329  

$x > 0$ (middle picture), now with polynomial reconstruction. On these frames are shown snapshot graphs with waves moving from left to right. We get a very nice looking numerical approximate solution with scheme (9)-(11), which in turn seems to be propagating at entirely entropy-correct Rankine-Hugoniot speed and similar good results are shown to the rarefaction case as well. Here, as the rarefaction wave is crossed, there is a sign change in the characteristic speed $u$ and thus there is one point at which $u = 0$, the sonic point. However, our numerical scheme now shows no spurious anomalies around $u = 0$. The classical nonlinear one-dimensional Buckley-Leverett case is depicted on the right picture in Figure 3 at time $t = 1$. These test cases here were simulated with 256 cells. Another example with the Buckley-Leverett flux function is seen on Figure 4, where we set a square wave as initial condition, $u(x, 0) = 1, -1 < x < 1$ and $u(x, 0) = 0$, otherwise (left picture). The solution profile starts as a rarefaction wave followed by a shock on the left side and a rarefaction wave followed by a shock on the right side for small times (middle picture). When the left shock meets the right rarefaction (see middle and right pictures in Figure 4), we observe the expected decaying pattern [10]; see also [5], Section 3.

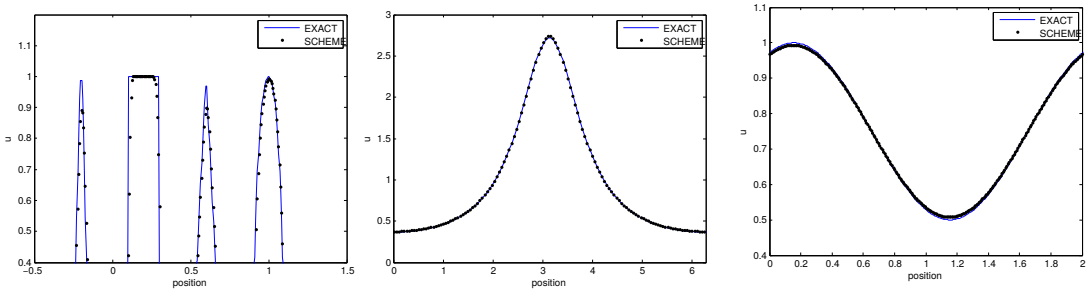


Figure 1: Left: Shu's linear test. Middle: Test case with $a(x, t) = \sin(x)$, the velocity is variable in space. Right: Test case with $a(x, t) = \sin(t)$, the velocity is variable in time.

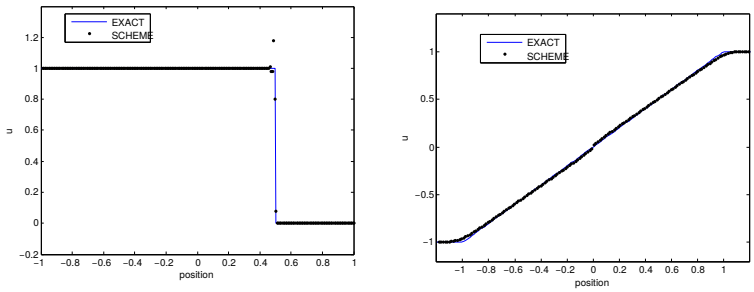


Figure 2: Nonlinear tests for Burgers' flux function without reconstruction. Left: shock wave, initial condition $u(x, 0) = 1, x < 0$ and $u(x, 0) = 0, x > 0$, end time $t = 0.5$. Right: rarefaction wave, $u(x, 0) = -1, x < 0$ and $u(x, 0) = 1, x > 0$, end time $t = 1.0$.

DOI: 10.5540/03.2017.005.01.0329

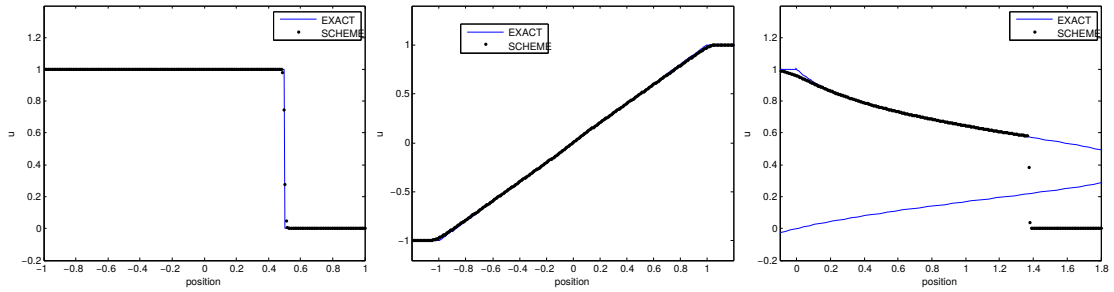


Figure 3: Nonlinear tests with reconstruction. Left: Burgers' flux function, shock wave solution with initial condition $u(x,0) = 1, x < 0$ and $u(x,0) = 0, x > 0$, end time $t = 0.5$. Middle: Burgers' flux function, rarefaction wave with initial condition $u(x,0) = -1, x < 0$ and $u(x,0) = 1, x > 0$, end time $t = 1.0$. Left: Buckley-Leverett flux function ($H(u) = u^2/(u^2 + 0.5(1-u)^2)$) with initial condition $u(x,0) = 1, x < 0$ and $u(x,0) = 0, x > 0$.

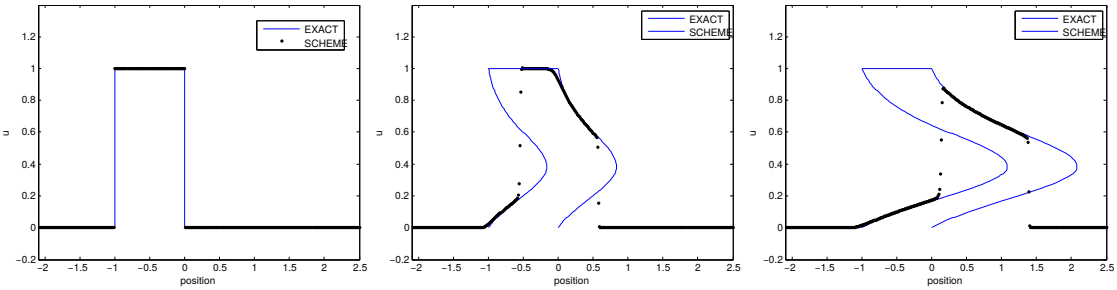


Figure 4: Buckley-Leverett flux function with initial condition $u(x,0) = 1, -1 < x < 1$ and $u(x,0) = 0$, otherwise. Snapshots at $t = 0$, $t = 0.4$ and $t = 1$, respectively.

## 4 Concluding Remarks

We presented the development of an effective numerical scheme for solving nonlinear scalar hyperbolic conservation laws problems with the Lagrangian-Eulerian framework. This method is based on a reformulation of the conservation laws in terms of an equivalent locally conservative space-time problem in divergence form. We make use of piecewise linear and parabolic reconstructions ideas for resolution and accuracy reasons and the resulting method present qualitatively correct numerical approximations. Our method is robust in a way that no special treatment is needed when the sign of velocity changes over time. We expect to establish a componentwise extension of the scheme in order to perform numerical experiments for systems of conservation and balance laws, as well as multidimensional problems. Our numerical experiments show good evidence of computational convergence.

DOI: 10.5540/03.2017.005.01.0329

## Acknowledgements

E. Abreu thanks for financial support through grants FAPESP No. 2014/03204-9, FAPESP No. 2011/23628-0, CNPq No. 445758/2014-7 and UNICAMP /FAEPEX No. 519.292-0280/2014. J. Perez and A. Santo thanks, respectively, CAPES-IMECC/ UNICAMP and CNPq-IMECC/ UNICAMP for a post-doctoral fellowship and a graduate fellowship.

## References

[1] E. Abreu. Numerical modelling of three-phase immiscible flow in heterogeneous porous media with gravitational effects. *Mathematics and Computers in Simulation*, 97:234–259, 2014.

[2] E. C. Abreu, W. Lambert, J. A. Perez S., and A. M. E. Santo. A lagrangian-eulerian algorithm for solving hyperbolic conservation laws with applications. In *Proceedings of the 6th International Conference on Approximation Methods and Numerical Modelling in Environment and Natural Resources (MAMERN VI)*, pages 599–617, Pau/Granada, 2015.

[3] J. Aquino, A. S. Francisco, F; Pereira, T. Jordem Pereira, and H. P. Amaral Souto. A lagrangian strategy for the numerical simulation of radionuclide transport problems. *Progress in Nuclear Energy*, 52(3):282–291, 2010.

[4] J. Douglas Jr, F. Pereira, and L.-M. Yeh. A locally conservative eulerian–lagrangian numerical method and its application to nonlinear transport in porous media. *Computational Geosciences*, 4(1):1–40, 2000.

[5] L. C. Evans *Partial differential equations* American Mathematical Society, 2010.

[6] C-S. Huang, T. Arbogast, and J. Qiu. An eulerian–lagrangian weno finite volume scheme for advection problems. *Journal of Computational Physics*, 231(11):4028–4052, 2012.

[7] G.-S. Jiang and C.-W. Shu. Efficient implementation of weighted eno schemes. Technical report, DTIC Document, 1995.

[8] R. J. LeVeque. *Finite volume methods for hyperbolic problems*, volume 31. Cambridge university press, 2002.

[9] H. Nessyahu and E. Tadmor. Non-oscillatory central differencing for hyperbolic conservation laws. *Journal of computational physics*, 87(2):408–463, 1990.

[10] O. A. Oleinik Discontinuous solutions of non-linear differential equations *Uspekhi Matematicheskikh Nauk* 12(3):3–73, 1957.

[11] J. A. Perez S. *Lagrangian-Eulerian approximate methods for balance laws and hyperbolic conservation law.* Tese de Doutorado, University of Campinas, 2015.

 